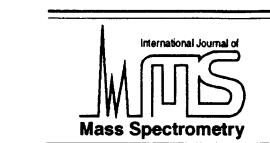




ELSEVIER

International Journal of Mass Spectrometry 210/211 (2001) 417–428



www.elsevier.com/locate/ijms

Beta cleavages of distonic ions, alpha cleavages of enol ions, isomerizations of distonic and enol ions and corresponding reactions of free radicals

Charles E. Hudson, David J. McAdoo*

Marine Biomedical Institute, University of Texas Medical Branch, 301 University Boulevard, Galveston, TX 77555-1069, USA

Received 4 December 2000; accepted 5 March 2001

Abstract

This study reports transition state energies for the losses of X from CH_2CHXZ and XCH_2CHZ ions and neutrals ($\text{X} = \text{H}$ or an alkyl radical, $\text{Z} =$ a functional group) and for 1,2-shifts by the same species. Ab initio methods were used to characterize methyl losses from $\text{CH}_3\text{CH}(\text{CH}_2)\text{C}(\text{OH})_2^+$ and $\text{CH}_3\text{CH}_2\text{CHC}(\text{OH})_2^+$. H shifts between and H losses from the alpha and beta carbons of $\text{C}_3\text{H}_6\text{O}_2^+$, and $\text{C}_3\text{H}_4\text{O}^{+}$ isomers and the corresponding reactions of ethyl and $\text{C}_2\text{H}_6\text{N}$ radicals were similarly characterized. Cleavage of bonds to the beta carbons of enolic and related species was found to be slightly more favorable energetically than dissociation from the alpha carbons of isomeric beta distonic ions and of beta radicals. However, dissociation from the alpha carbons of beta distonic radical cations probably also occurs at suprathreshold energies, but at a lower rate than the competing dissociation from the beta carbons of isomeric radical cation enols. Critical energies are similar for corresponding dissociations of the ions and neutrals. Finally, 1,2-shifts in radical cations, including shifts of functional groups, have substantially lower critical energies than do the corresponding reactions of neutral free radicals such that the ions but not the free radicals can isomerize below their dissociation thresholds. In summary, the presence of a charged group appears to facilitate the interconversion of enolic and beta distonic radical cations by 1,2-shifts, but not dissociation of those ions. (Int J Mass Spectrom 210/211 (2001) 417–428) © 2001 Elsevier Science B.V.

Keywords: Distonic ions; enol ions; Free radicals; Isomerization; ab initio

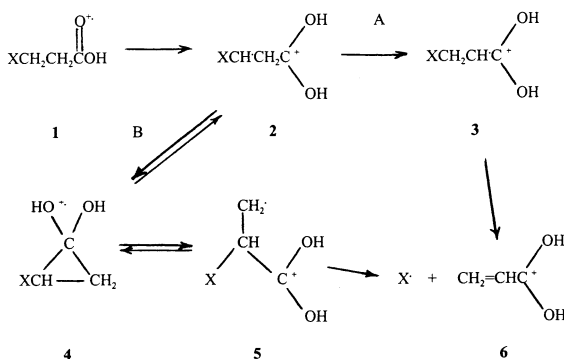
1. Introduction

We are pleased to have this opportunity to honor Nico Nibbering for his many contributions to mass spectrometry and gas phase ion chemistry across the past several decades. To this end, we present an ab initio study of reactions related to 1,2-shifts and

dissociations of the butanoic acid ion that we studied experimentally years ago in collaboration with Nibbering and co-workers [1,2]. In those studies we proposed that the dissociations of the butanoic acid ion include reactions corresponding to pathway B in Scheme 1 [1]. (In the scheme $\text{X} = \text{H}$ or an alkyl radical.) However, other investigators soon concluded that losses of radicals from ionized carboxylic acids and related ions occur exclusively from their enol forms [Scheme 1 (A)]; i.e., dissociation from the isomeric β -distonic ions [Scheme 1(B)] is negligible

* Corresponding author. E-mail: djmcadoo@utmb.edu

Dedicated to Professor Nico Nibbering on the occasion of his retirement.



[3–6]. We also proposed that alpha–beta H transfer is facilitated by the presence of the charge [2], as opposed to being a purely radical reaction (such reactions are highly unfavorable in free radicals [7]. In support of the latter conclusion, it was inferred [6] that the reaction preference in the dissociations of ions is related to the exclusive addition of alkyl radicals to the beta carbons of substituted olefins in solution [8]. However, subsequent ^{13}C labeling results and Rice-Ramsperger-Kassel-Marcus calculations implied that pathway B as well as pathway A of Scheme 1 is active in the dissociations of the methyl butanoate ion [9]. In light of the disparate conclusions regarding whether type B dissociations can compete with type A dissociations and the difficulties in resolving the issue experimentally, we characterized type A and B reactions in an assortment of systems by contemporary ab initio theory.

2. Theory

Calculations were performed with the GAUSSIAN 94 package [10] on a Cobra Corra Alpha computer or the GAUSSIAN 98 package [11] on a Dell Dimension 4100 PC with an Intel Pentium III processor. Ground state geometries were identified in all cases as minimum energy points having only real vibrational frequencies. All transition states described had only one imaginary frequency. Ground state and transition state geometries were located with MP2/6-31G(*d*) frozen core theory, and vibrational frequencies and force

constants were calculated for those points. From the resulting geometries and force constants the stationary points were located at the QCISD/6-31G(*d*) level. All vibrational frequencies were obtained from MP2/6-31G(*d*) theory and were multiplied by 0.9670 when used for zero point vibrational energy corrections [12]. At the ultrahigh frequency level, all of the transition states for dissociations had high $\langle s^2 \rangle$ values in the range 0.94–1.0; the $\langle s^2 \rangle$ values for the isomerization transition states were 0.79–0.82, and values for the ground state species were very close to 0.76, except the value for CH_3CHCO^+ was 0.80. The value of $\langle s^2 \rangle$ in the absence of spin contamination is 0.75. However, QCISD/6-311G(*d,p*) and QCISD(T)/6-311G(*d,p*) energies (QCISD = quadratic configuration interaction singles doubles) were within a few kJ/mol^{-1} of PMP3/6-311G(*d,p*) energies (results with spin contamination projected out) for the problem systems (Table 1). Thus spin contamination did not appear to substantially affect the energies we obtained at the highest levels of theory we applied.

Some of the distonic ions studied have multiple possible conformations. In all of these cases, multiple conformations of the ion were examined, and the results reported are for the most stable conformation found.

3. Results and Discussion

3.1. $\text{C}_4\text{H}_8\text{O}_2^+$ isomers

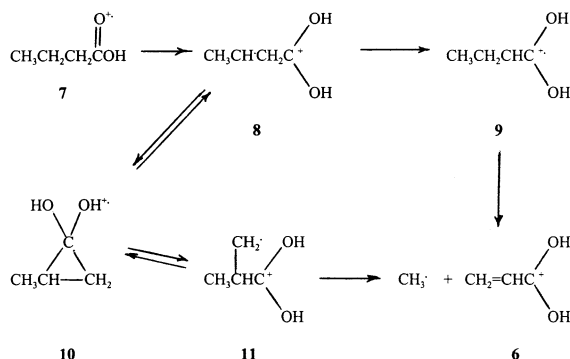
The loss of methyl from ionized butanoic acid follows five-membered ring H transfer from the beta carbon to the carboxyl group and H-transfer from the alpha to the beta carbon (Scheme 2) [1,2,13,14]. It is also clear that there is some skeletal isomerization to **11** as in pathway B. However, whether some methyl is lost directly from the distonic intermediate **11** has not previously been examined, even though it is clear that **11** is accessed. Therefore, we used ab initio computations (Table 1) to define better the details of how pertinent isomers of the butanoic acid ion dissociate.

Table 1

Energies for radical cations, free radicals, and their reactions ($H^\bullet = 218 \text{ kJ mol}^{-1}$)

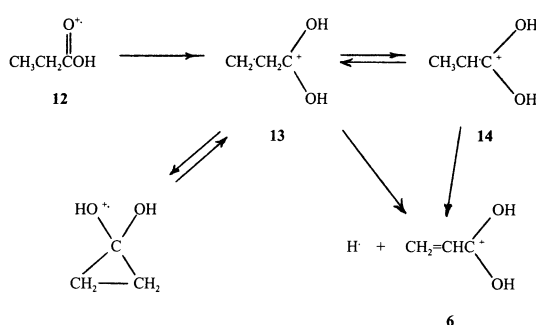
Structure	QCISD	PMP3	E[QCISD(T)]	ZPVE	E_{rel}	QCISD(T)	$\Delta_f H(\text{exp})^a$
$\text{CH}_3\text{CH}_2\text{CH}_2\text{CO}_2\text{H}^{\bullet+}$ (7) ^b							507
$\text{CH}_3\text{CH}_2\text{CHC}(\text{OH})_2^{\bullet+}$ (9) ^b	−306.598 739	−306.579 394	−306.629 331	307.2	−39.9		
$\text{CH}_3\text{CH}(\text{C}(\text{H}_2)_2)\text{C}(\text{OH})_2^{\bullet+}$ (11) ^b	−306.581 475	−306.562 629	−306.612 306				
TS(11 → 6) ^b	−306.534 373	−306.518 560	−306.567 069	293.7	110.1		
TS(9 → 6) ^b	−306.543 548	−306.525 016	−306.573 375	292.7	92.5		
$\text{CH}_2=\text{CHC}(\text{OH})_2^{\bullet+}$ (6) ^c	−266.879 830	−266.864 898	−266.910 091				
$6^{\bullet+} + \text{CH}_3^{\bullet}$	−306.539 832	−306.519 891	−306.570 800	282.8	89.4		
$\text{CH}_3\text{CH}_2\text{CO}_2\text{H}^{\bullet+}$ (12)	−267.415 665	−267.399 393	−267.442 983	231.0	58.8		567
$\text{CH}_2\text{CH}_2\text{C}(\text{OH})_2^{\bullet+}$ (13) ^c	−267.437 175	−267.422 928	−267.464 498	228.7			
$\text{CH}_3\text{CHC}(\text{OH})_2^{\bullet+}$ (14) ^c	−267.458 183	−267.443 744	−267.485 580	231.2	−52.9		437
TS(12 → 13)	−267.398 150	−267.380 639	−267.428 707	221.9	87.2		
TS(13 → 13') ^c	−267.400 293	−267.386 248	−267.430 158	228.6	90.1		
TS(13 ⇌ 14) ^c	−267.393 899	−267.381 647	−267.423 610	220.4	99.1		
TS(13 → 6) + H) ^c	−267.370 106	−267.358 024	−267.400 146	210.6	150.9		
TS(14 → 6 + H) ^c	−267.406 410	−267.363 132	−267.406 410	211.6	135.4		
6 + H ^c	−267.379 639	−267.364 707	−267.409 900	205.3	119.9		
$\text{CH}_2\text{CH}_2\text{CH}=\text{OH}^{\bullet+}$ (17) ^c	−192.322 958	−192.310 988	−192.343 768	215.2	0		
$\text{CH}_3\text{CHCHOH}^{\bullet+}$ (19) ^c	−192.354 129	−192.342 756	−192.374 860	219.8	−77.0		665
TS(19 → 20) ^c	−192.289 619	−192.278 840	−192.311 300	208.0	78.2		
TS(17 → 19) ^c	−192.297 836	−192.288 662	−191.320 844	210.3	55.3		
TS(20 → 18 + H) ^c	−192.261 871	−192.251 906	−192.285 453	198.9	136.8		
TS(19 → 18 + H) ^c	−192.267 305	−192.257 190	−192.291 215	199.3	122.1		
$\text{CH}_2=\text{CHCH}=\text{OH}^{\bullet+}$ (18) ^c							642
18 + H ^c	−192.269 657	−192.257 713	−192.293 787	193.4	109.4		860
$\text{CH}_2\text{CH}_2\text{CO}^{\bullet+}$ (21) ^c	−191.121 005	−191.105 178	−191.143 762	152.8	0		756
$\text{CH}_3\text{CHCO}^{\bullet+}$ (22) ^c	−191.137 328	−191.122 685	−191.160 415	157.7	−38.8		
TS(21 → 21') ^c	−191.092 865	−191.078 341	−191.117 658		68.5 ^d		
TS(21 → 22) ^c	−191.070 602	−191.056 739	−191.096 154	146.0	118.2		
TS(21 → 23 + H) ^c	−191.048 420	−191.034 858	−191.074 105	136.7	166.8		
TS(22 → 23 + H) ^c	−191.056 410	−191.041 717	−191.082 299	137.8	146.4		
$\text{CH}_2=\text{CHCO}^{\bullet+}$ (23) ^c							751
23 + H ^c	−191.059 432	−191.042 454	−191.085 400	130.4	130.8		969
$\text{CH}_3\text{CH}_2^{\bullet}$ (24) ^c	−78.938 245	−78.934 022	−78.946 757	156.0	0		118
TS(24 → 24') ^c	−78.864 949	−78.861 584	−78.875 452	146.5	177.1		
TS(24 − H) ^c	−78.867 268	−78.863 421	−78.878 495	139.3	162.5		
$\text{CH}_2=\text{CH}_2^{\bullet}$	−78.327 897	−78.367 388	−78.384 225				52.2
$\text{CH}_2=\text{CH}_2 + \text{H}^{\bullet}$	−78.872 706	−78.867 197	−78.884 034	132.1	140.8		270.2
$\text{CH}_2\text{CH}_2\text{NH}_2^{\bullet}$ (25) ^c	−134.158 350	−134.151 785	−134.173 494	203.8	0		
$\text{CH}_3\text{CHNH}_2^{\bullet}$ (26) ^c	−134.173 171	−134.166 122	−134.188 473	203.1	−40.0		
TS(25 → 28) ^c	−134.092 768	−134.088 509	−134.110 555	185.3	146.7		
TS(26 → 28) ^c	−134.100 927	−134.094 899	−134.119 074	185.9	125.0		
TS(25 ⇌ 26) ^c	−134.089 586	−134.084 170	−134.106 615	193.3	165.1		
$\text{CH}_2\text{CH}_2\text{NH}_2^{\bullet}$	−134.043 356	−134.035 995	−134.063 934	181.7	309.7		
TS(25 → $\text{CH}_2=\text{CH}_2 \dots \text{NH}_2$)	−134.116 287	−134.110 898	−134.133 394	196.7	112.4		
$\text{CH}_2=\text{CHNH}_2$ (28)	−133.603 831	−133.596 984	−133.621 743				
$\text{CH}_2=\text{CHNH}_2 + \text{H}^{\bullet}$	−134.103 640	−134.096 793	−134.121 552	178.4	111.0		

^aResults obtained with a 6-311G(d,p) basis set and QCISD/6-31G(d) geometry.^bFrom [25].^cResults obtained with a 6-311G(d) basis set and QCISD/6-31G(d) geometry.^dLacking ZPVE corrections because ZPVE could not be determined because the species is not stable at the levels (MP2 and B3LYP) of theory that have analytical frequency calculations.^eThis is a transition state for H loss from N.



Transition states were located for losses of methyl from both the branched beta dicarbonyl ion (**11**) and the enol isomer of ionized butanoic acid (**9**). The energy of TS(**9** → **6**) was only 3.1 kJ mol⁻¹ above that of the dissociation products **6** + CH₃, demonstrating at most a very small critical energy for the corresponding reverse reaction. The QCISD(T) threshold for **11** → **6**, dissociation of a dicarbonyl isomer, was 17.6 kJ mol⁻¹ higher than that for dissociation of the enol **9** to the same products. Thus the critical energy for addition to the beta carbon is higher than that for addition to the alpha carbon, but still not very substantial. Therefore **9** → **6** would be expected to be strongly dominant in metastable dissociations. The relative contributions of the two reactions would depend on the fractions of **11** and **9** present as well as their transition state energies. The concentration of **11** would be expected to be high early in the course of evolution over Scheme 2 because skeletal isomerizations such as **8** → **10** → **11** typically have lower thresholds than reactions analogous to **8** → **9** (see sec. 3.2). Thus **11** → **6** could well be comparable in degree to **9** → **6** in dissociations at short times, in contrast to previous conclusions [3–6].

Although their relative order is the same, present reverse critical energies (3.1 and 17.6 kJ mol⁻¹) are substantially lower than those found previously for analogous reactions by MNDO theory (previous values for the methyl butanoate ion: 79 kJ mol⁻¹ for the dissociation step in A and 121 kJ mol⁻¹ for the same step in B [4], and for ionized 2-methylbutanoic acid the corresponding values are 74 and 113 kJ mol⁻¹ [5].



It was argued in earlier work that additions of radicals to protonated, unsaturated acids like **6** would preferentially give the enol products because the enol products are much more stable than isomeric dicarbonyl isomers [6]. Our calculations do confirm that **9** is more stable than **11**, so relative reactant stability could contribute to transition state (**9** → **6**) being slightly lower in energy than TS(**11** → **6**), as will be discussed further.

3.2. C₃H₆O₂⁺ Isomers

The propanoic acid ion (**12**) produces **6** by losing H originally from both its alpha and beta positions [15], making it a useful model for the purposes of the present study. Relevant reactions of this system are summarized in Scheme 3.

The decomposition patterns of C₃(H,D)₆O₂⁺ ions demonstrate at least a slight preference for H loss from **12** in the ion source by CH₃CHC(OH)₂⁺ (**14**) → **6**, but do not rule out a significant portion taking place by CH₂⁺CH₂C(OH)₂⁺ (**13**) → **6** [15]. Whether the losses of both alpha and beta hydrogens reflect fragmentations from both **13** and **14** or only from **14** following hydrogen shuffling or carboxyl shifting cannot be resolved experimentally, so we examined the reactions of those ions by theory. Ab initio energies for the interconversion of **13** and **14**, losses of H[•] from those ions, and other pertinent reactions are given in Table 1. The ab initio geometries for the reactants and the transition states for C₃H₆O₂⁺ reactions of interest are given in Figs. 1–5, and a potential energy diagram based on the ab initio energies is

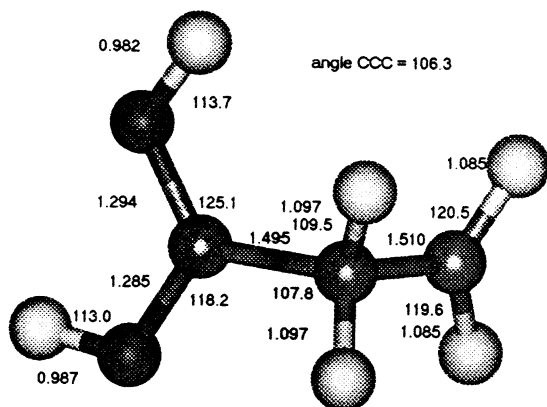


Fig. 1. Geometry of $\text{CH}_2\text{CH}_2\text{C}(\text{OH})_2^+$ (**13**) obtained by QCISD/6-31G(d) ab initio theory.

given in Fig. 6. As in related earlier MNDO studies [4,5], the ab initio threshold for H^\cdot loss from **13** is higher than that for H^\cdot loss from **14**. Further, both thresholds for dissociation are well above the transition state energies for $\mathbf{12} \rightarrow \mathbf{13}$, $\mathbf{13} \rightarrow \mathbf{14}$ and the degenerate carboxyl shift $\mathbf{13} \rightarrow \mathbf{13}'$. (For $\text{C}_3\text{H}_6\text{O}_2^+$, not all possible configurations of the cyclopropanediol-like transition state were examined, so it is possible that there is slightly lower energy pathway for a 1,2-protonated carboxyl shift. A stable ionized cyclopropanediol could not be located, suggesting that such species are too strained to be stable minima.) Thus, in principle **13** and **14** can interconvert and H^\cdot be lost from either structure at higher energies. In

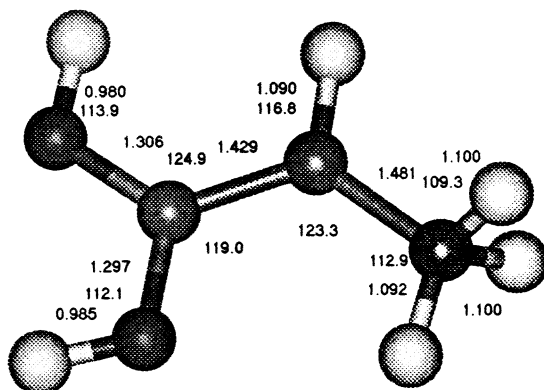


Fig. 2. Geometry of $\text{CH}_3\text{CHC}(\text{OH})_2^+$ (**14**) obtained by QCISD/6-31G(d) ab initio theory.

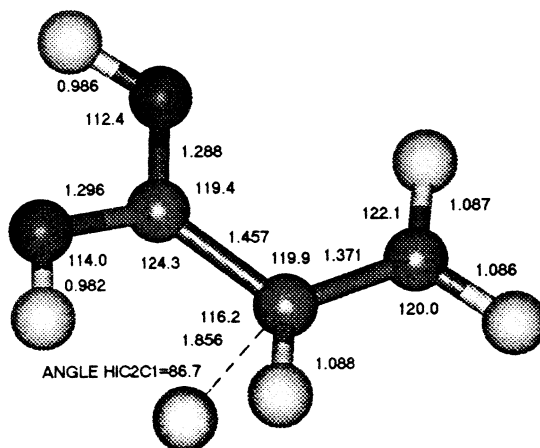


Fig. 3. Geometry of $\text{TS}(\mathbf{13} \rightarrow \text{CH}_2=\text{CHC}(\text{OH})_2^+ + \text{H})$ obtained by QCISD/6-31G(d) ab initio theory.

particular, following $\mathbf{12} \rightarrow \mathbf{13}$ at suprathreshold energies, $\mathbf{13} \rightarrow \mathbf{6}$ might compete effectively with $\mathbf{14} \rightarrow \mathbf{6}$. However, these results are also consistent with $\mathbf{14} \rightarrow \mathbf{6}$ being the dominant, perhaps only, metastable decomposition between the two processes.

Both H^\cdot losses have reverse barriers (15 kJ mol^{-1} for $\mathbf{6} + \text{H}^\cdot \rightarrow \mathbf{14}$ and 31 kJ mol^{-1} for $\mathbf{6} + \text{H}^\cdot \rightarrow \mathbf{13}$), small but somewhat higher than those for the dissociations of the above $\text{C}_4\text{H}_8\text{O}_2^+$ isomers. The results also confirm that **14** is more stable than **13**, so, as for the $\text{C}_4\text{H}_8\text{O}_2^+$ isomers, relative reactant stability could be a factor causing $\text{TS}(\mathbf{14} \rightarrow \mathbf{6})$ to be slightly lower in

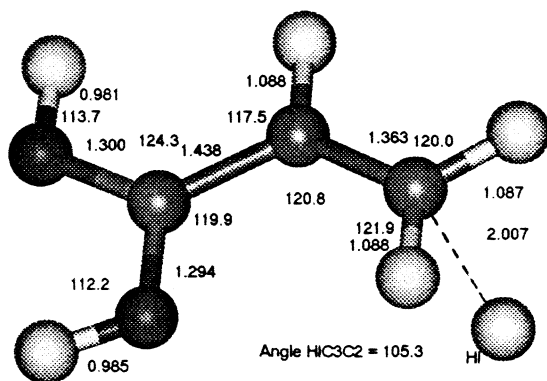


Fig. 4. Geometry of $\text{TS}(\mathbf{14} \rightarrow \text{CH}_2=\text{CHC}(\text{OH})_2^+ + \text{H})$ obtained by QCISD/6-31G(d) ab initio theory.

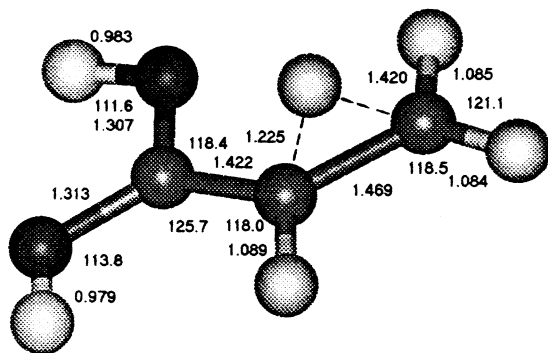


Fig. 5. Geometry of TS(**13** \leftrightarrow **14**) obtained by QCISD/6-31G(*d*) ab initio theory.

energy than TS(**13** \rightarrow **6**), in turn influencing the preference between the two reactions.

The occurrence of both dissociations is also reasonable in light of the transition state geometries (Fig. 1 and 2). In both transition states the H is situated well above the plane of the incipient **6**. The departing H is slightly further from the carbon of its origin in TS(**14** \rightarrow **6**) (2.007 Å) than in TS (**13** \rightarrow **6**) (1.8564 Å). The geometries of these transition states suggest a reason

for the slightly higher threshold for the dissociation of **13**: the CCC(O)O skeleton is slightly twisted in that transition state, whereas it is planar for **14**, **6**, and TS(**14** \rightarrow **6**). The HCCC dihedral angles involving hydrogens of the incipient methylene deviate 8.0° and 12.2° from planarity in **13** versus deviations of 5.2° and 4.8° from planarity in **14**. The twisted geometry, i.e. earlier transition state, of TS(**13** \rightarrow **6**) is probably related to the lower critical energy of **13** \rightarrow **6** + H \cdot (151 kJ mol⁻¹) relative to that for **14** \rightarrow **6** + H \cdot (173 kJ mol⁻¹), which may in turn stem from the difference between the stabilities of the reactants dissociating to a common product. The high critical energy for the dissociation of **14** permits the CH bond to break to the extent that at the transition state the incipient CH₂=CHC(OH)₂⁺ is close to the geometry of **6**. However, if it took the same amount of energy to break the CH bond in the dissociation of **13**, that would elevate the corresponding transition state energy well above that of the products. Given that **13** is 52.9 kJ mol⁻¹ higher in energy than **14** and TS(**13** \rightarrow **6**) is only 15.5 kJ mol⁻¹ above TS (**14** \rightarrow **6**), it appears that the transition state energy for **13** \rightarrow **6** is

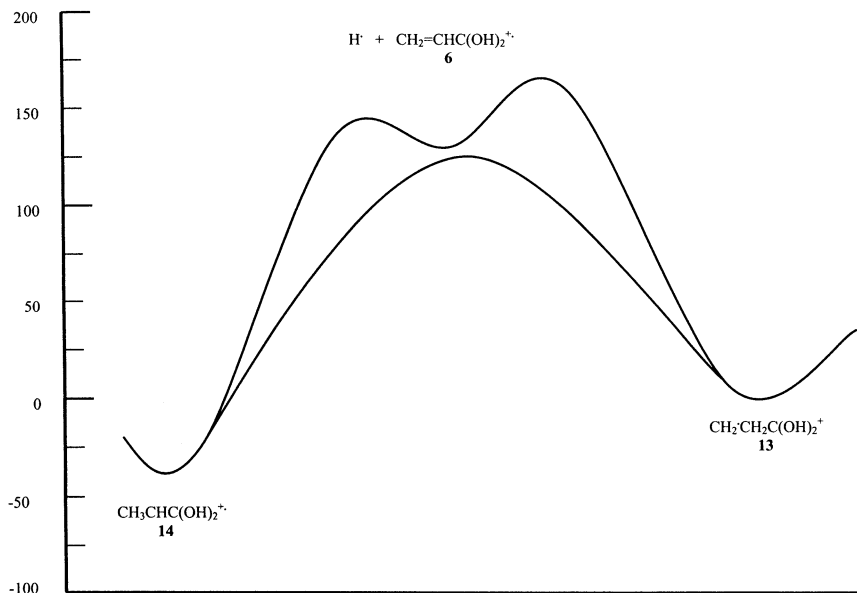


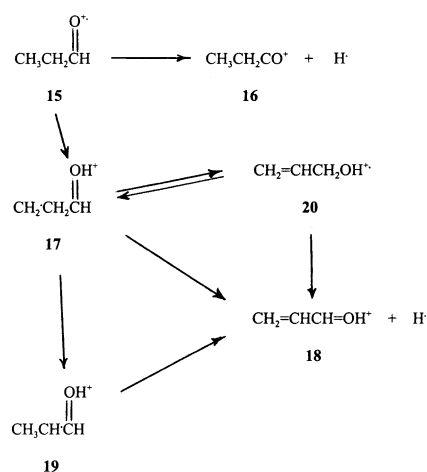
Fig. 6. Potential energy surface for interconversions and dissociations of CH₂CH₂C(OH)₂⁺ (**13**) and CH₃CHC(OH)₂⁺ (**14**) based on relative energies at the QCISD(T)/6-311G(*d,p*)/QCISD/6-31G(*d*) + ZPE level of theory.

raised above the product heats of formation by the energy required to break the CH bond.

Weiske and Schwarz [6] suggested that preferential attack on C_β rather than C_α of protonated, conjugated substituted olefins such as **6** is related to nucleophilic properties of free radicals. $H\cdot$ is nonpolar and has a very low polarizability, so nucleophilicity is not very important in addition by $H\cdot$. Consistent with nucleophilicity being important in determining the site of addition, there is substantially more positive charge on C_β than on C_α in both transition states for $H\cdot$ loss from $C_3H_6O_2^{+\cdot}$ ions when the net charges on the C's and attached H's are summed in a Mulliken population analysis (0.25 versus 0.005 positive charges on C_β versus C_α for the transition state for dissociation from **13** with corresponding values of 0.26 versus 0.04 for dissociation from **14**). However, this is in some measure due to the extra H on C_β because substantial positive charge is placed on H in Mulliken population analysis (0.25–0.27 on H's fully bonded to C in **13** and **14**). When the charge assigned to the carbons alone is considered, the carbon from which the $H\cdot$ is departing is most negatively charged, more so in **14** (–0.33 versus –0.22) than in **13** (–0.30 versus –0.26). The **13**–**14** difference is opposite from what would be expected if the nucleophilicity of the radical is important. Although Mulliken analysis does not enable us to clearly address whether the nucleophilicity of the departing radical is important in establishing the preferred dissociation pathway, the low nucleophilicity of the H atom argues against it.

3.3. $C_3H_6O^{+\cdot}$ isomers

The dissociations of distonic (**17**) and enolic (**19**) $C_3H_6O^{+\cdot}$ species are the simplest possible A and B type dissociations. However, $H\cdot$ losses from metastable $C_3H_6O^{+\cdot}$ ions produce $CH_3CH_2CO^+$ rather than $CH_2=CHCH=OH^+$ [16–18], so neither of the reactions of interest is the lowest energy $H\cdot$ loss from $C_3H_6O^{+\cdot}$ ions. However, at higher energies some $CH_2=CHCHOH^+$ is formed by the loss of $H\cdot$ from ionized allyl alcohol (**20**) [16,17] and from the enol isomer **19** [19]. The interconversions and loss of $H\cdot$



Scheme 4.

from $C_3H_6O^{+\cdot}$ ions with the skeletal structure CCCO, excluding **17** \rightarrow **18** and **19** \rightarrow **18**, have already been characterized in detail by theory [18]. (See Scheme 4)

Unfortunately, rather than directly losing $H\cdot$, in our ab initio studies the distonic ion **17** isomerizes to and loses $H\cdot$ from **20**. The transition state energy for this dissociation is probably very close to the threshold for **17** \rightarrow **18** + $H\cdot$ { **13** \rightarrow **6** + $H\cdot$ } is 31 kJ mol⁻¹ above $\Delta_f H(\mathbf{6} + \text{H}\cdot)$, whereas TS(**20** \rightarrow **18** + $H\cdot$) is 27.4 kJ mol⁻¹ above $\Delta_f H(\mathbf{18} + \text{H}\cdot)$. Thus comparing the theoretical threshold for loss of $H\cdot$ from **20** (136.8 kJ mol⁻¹) to that for **19** \rightarrow **18** + $H\cdot$ (122.1 kJ mol⁻¹) suggests that the threshold for loss of $H\cdot$ from distonic **17** would be about 15 kJ mol⁻¹ higher than that for the same dissociation of the enol **19**. However, no further conclusions pertinent to the aims of the present study can be drawn from the data for the $C_3H_6O^{+\cdot}$ isomers. Our results do support previous conclusions [16,18,19] that **17**, **19**, and **20** interconvert extensively at and below their threshold for dissociation.

3.4. $C_3H_4O^{+\cdot}$ ions

The dissociations of the $C_3H_4O^{+\cdot}$ isomers $CH_2^+\text{CH}_2\text{CO}^+$ (**21**) and $CH_3\text{CH}^+\text{CO}^+$ (**22**) were also characterized to see if the factors that operate in the dissociation of enols versus their distonic isomers also operate in nonenolic unsaturated radical cations. The energies in Table 1 and in the potential energy

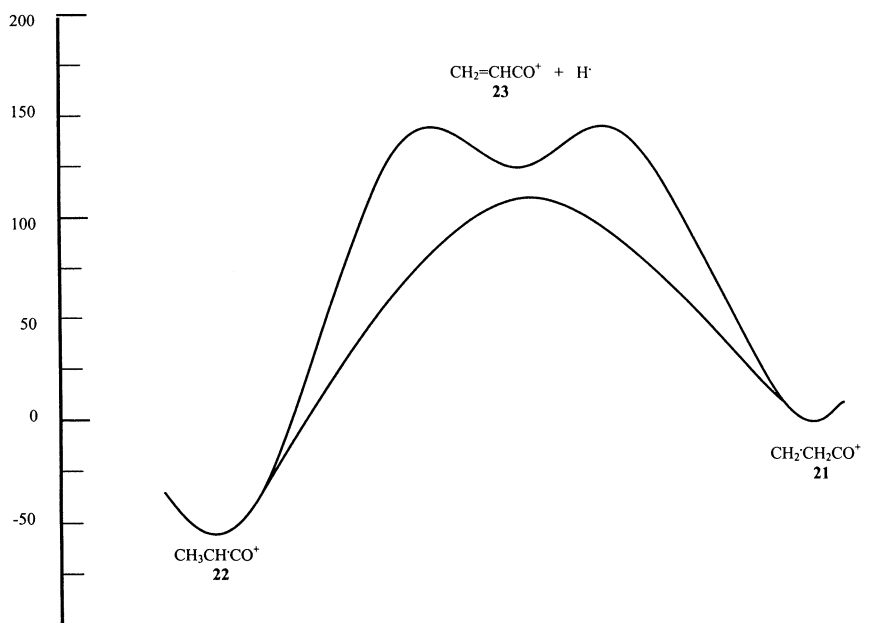
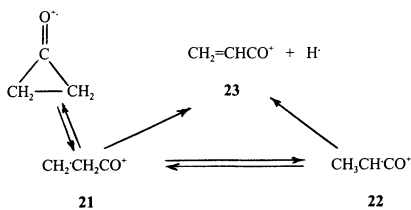


Fig. 7. Potential energy surface for interconversions and dissociations of $\text{CH}_2\text{CH}_2\text{CO}^+$ (**21**) and CH_3CHCO^+ (**22**) based on relative energies at the QCISD(T)/6-311G(d,p)/QCISD/6-31G(d) + ZPE level of theory.

diagram in Fig. 7 demonstrate that for this system, in parallel to the above enol versus distonic systems, **22** is more stable than **21**. The 38.8 kJ mol^{-1} difference obtained between the heats of formation of the two ions by present theory agrees very well with a 36 kJ mol^{-1} difference previously obtained by more primitive theory [20]. There is also good agreement with a heat of formation of **21** of 803 kJ mol^{-1} obtained by B3LYP/3-21G(d) theory [21]. (See Scheme 5.)

There is a significant barrier to interconversion of **21** and **22**. As with the enol ions and their isomers, the energy of $\text{TS}(\mathbf{21} \rightleftharpoons \mathbf{22})$ is below those for dissociation from **21** or **22**. These data are consistent with a

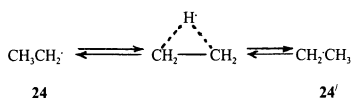


Scheme 5.

previous conclusion [20] that nondissociating **21** and **22** largely maintain their identity. However, they also allow those two isomers to interconvert below their thresholds for H loss. Effective hydrogen repositioning by way of the degenerate 1,2-CO shift is predicted to be facile by its transition state being about 50 kJ mol^{-1} lower in energy than that for $\text{TS}(\mathbf{21} \rightarrow \mathbf{22})$. $\text{TS}(\mathbf{21} \rightarrow \mathbf{21})$ is a transition state rather than a stable cyclopropanone ion at the higher levels of theory applied, suggesting that, as with ionized cyclopropanediol, ionized cyclopropanone is too strained to be a stable species.

The relative energies of the characterized points on the $\text{C}_3\text{H}_4\text{O}^{++}$ potential surface are similar to those for the corresponding species on the $\text{C}_3\text{H}_6\text{O}_2^{++}$ and $\text{C}_3\text{H}_6\text{O}^{++}$ surfaces, suggesting that the same factors determine the corresponding transition state energies in all of those systems.

The CH distance in the breaking bond in $\text{TS}(\mathbf{21} \rightarrow \mathbf{23})$ was 1.856 \AA , whereas that in $\text{TS}(\mathbf{22} \rightarrow \mathbf{23})$ was 2.002 \AA . As for **13** and **14**, the methylene in the



Scheme 6.

dissociating **21** was less planar (HCCC dihedral angles 13.8°–13.9°) than that developing during the dissociation of **22** (HCCC dihedral angles about 5°). Thus again greater transition state planarity is associated with a higher critical energy.

3.5. $\text{CH}_3\text{CH}_2\cdot$

We also examined reactions of two neutral radicals to enable us to compare 1,2-H shifts and direct H[•] losses in charged versus uncharged radicals. As noted above, free radical addition to conjugated olefins occurs exclusively on the beta carbon [8], the reverse of pathway A. The reactions of the ethyl radical (**24**) were characterized as prototypes of 1,2-H shifts and H[•] losses from positions adjacent to the formal radical site by free radicals. This radical does not have an isomer corresponding to an enolic radical cation, so its reactions correspond more to those of the distonic radical cations. (See Scheme 6.)

Three features of the dissociations of **24** are to be noted (1). Theory produced a threshold for H[•] loss (162.5 kJ mol⁻¹) similar to those for H[•] losses from the distonic radical cations (151 kJ mol⁻¹ for **13** and 167 kJ mol⁻¹ for **21**). The reverse critical energy (21.7 kJ mol⁻¹) for dissociation was also similar to those from the distonic ions. (2) In contrast to the radical cations, more energy is required for a 1,2-H shift in the ethyl radical than for H[•] loss from it. This is in qualitative agreement with earlier ab initio studies of this isomerization [7,22]. (3) Isomerization of **24** requires substantially more energy (177 kJ mol⁻¹) than do the 1,2-H shifts in radical cations (the mean of the critical energies of the radical cation isomerizations studied here is 91 kJ mol⁻¹). Also, the hydrogens in the incipient methylene formed HCCH dihedral angles of 5.6°–9.7° in the transition state for dissociation, closer to those for dissociations of dis-

tonic than enolic ions. The CH distance in the transition state for breaking the CH bond is 1.902 Å.

Differing conclusions have been presented as to whether 1,2-shifts in radical cations are purely radical reactions [6] or whether the charge facilitates them [22,23]. The higher critical energy for 1,2-shifts in **24** than in the radical cations is consistent with the charge facilitating the corresponding reactions in radical cations.

3.6. $\text{C}_2\text{H}_6\text{N}\cdot$

Finally, we characterized the reactions of $\text{CH}_2\text{CH}_2\text{NH}_2$ (**25**) and $\text{CH}_3\text{CH}\cdot\text{NH}_2$ (**26**) to enable us to compare further 1,2-H shifts in radical cations to the corresponding reactions of a radical. A potential energy diagram is given in Fig. 8 and ab initio transition state geometries for H[•] losses from **25** and **26** in Figs. 9 and 10. As for the ethyl radical, the thresholds for H[•] loss and the barriers to the reverse reactions were comparable to those for the corresponding dissociations of radical cations. Also as for the ethyl radical and in contrast to the radical cations, the critical energy for isomerization was substantially above those for H[•] loss from the two isomers. This is further evidence that the presence of a positive charge lowers the critical energy for 1,2-shifts between alpha and beta carbons during the interconversion of enolic and beta distonic radical cations. (See Scheme 7.)

In the transition states the departing H[•] was 1.776 Å from its carbon for **25** and 1.940 Å from its carbon for **26**. In contrast to the distonic versus isomeric ions above, the former transition state was perhaps more planar (HCCN dihedral angles 1.1° and 10.6°) than the latter (HCCN dihedral angles 7.2°–11.2°).

Efforts were made to find a transition state for the 1,2-NH₂ shift **25** → **25'**. A symmetric, three-membered ring structure was located that appeared to be a transition state leading to H[•] loss from N to form $\overline{\text{CH}_2\text{CH}_2\text{NH}}$. The symmetric transition state would not be expected to be stable because it would violate the electron octet of nitrogen. Another transition state was located that appeared to be a transition state for **25** → **27'**, where **27** consists of an NH₂ H bonded to the middle of the double bond of ethylene (Fig. 11),

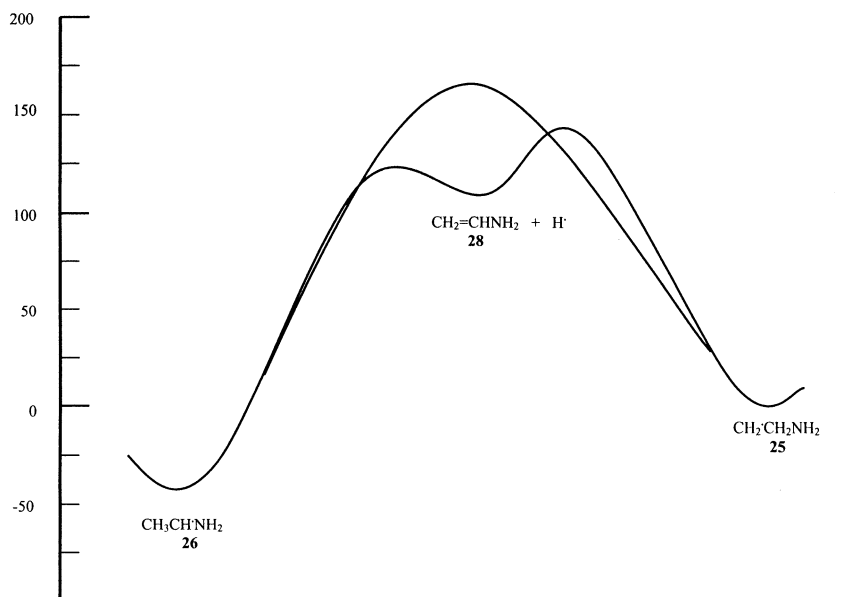


Fig. 8. Potential energy surface for interconversions and dissociations of $\text{CH}_2\text{CH}_2\text{CNH}_2$ (**25**) and CH_3CHNH_2 (**26**) based on relative energies at the QCISD(T)/6-311G(*d,p*)/QCISD/6-31G(*d*) + ZPE level of theory.

thereby altogether avoiding $[\text{CH}_2\text{CH}_2\text{NH}_2]^\ddagger$. Thus **25** \rightarrow **27** appears to be more a dissociation addition than a 1,2-shift with simultaneous bond breaking and making. However, **27** itself was never completely optimized, so whether it could be an intermediate in $\text{25} \rightleftharpoons \text{25}'$ is not resolved.

4. Conclusions

We conclude the following from results obtained in this work.

- (1) Dissociation from the alpha carbons of β -distrionic cations probably occurs, but at a lower rate than the corresponding dissociation from the beta car-

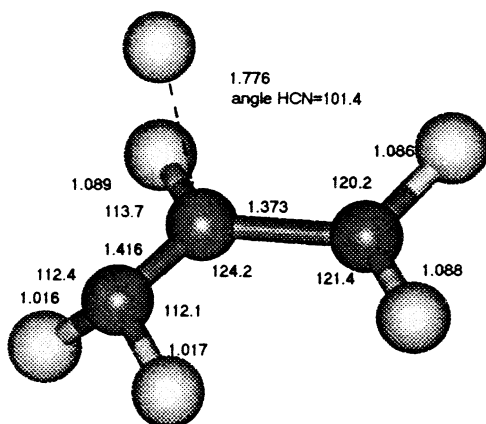


Fig. 9. Geometry of TS(**25** \rightarrow **28**) obtained by QCISD/6-31G(*d*) ab initio theory.

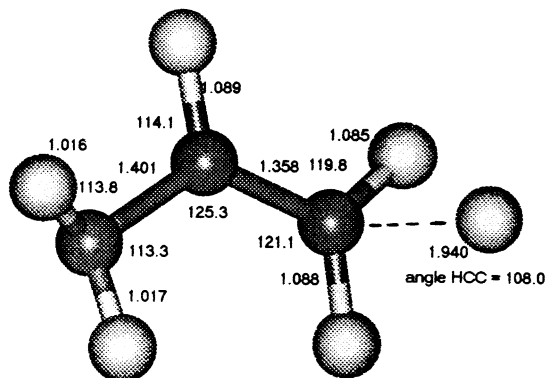
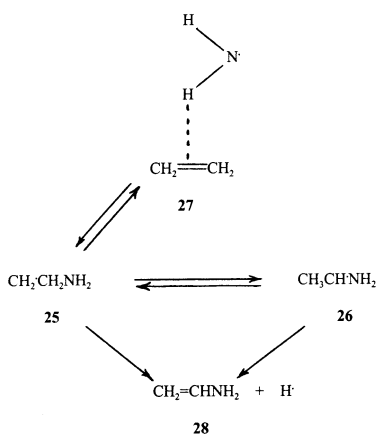


Fig. 10. Geometry of TS(**26** \rightarrow **28**) obtained by QCISD/6-31G(*d*) ab initio theory.



bon of isomeric enol radical cations.

- (2) Dissociation from the beta carbons of enolic ions, corresponding forms of other radical cations and free radicals is more, but only slightly more, favorable energetically than is dissociation from the alpha carbon of isomeric beta distonic ions/beta radicals.
- (3) The presence of the charge appears to facilitate the interconversion of enolic and beta distonic radical cations by 1,2-H shifts.
- (4) Neutral free radicals dissociate more readily than they undergo 1,2-H shifts, consistent with Walling's model placing one of the three electrons involved in bond breaking and making in a 1,2-shift in a high-lying antibonding orbital [24].

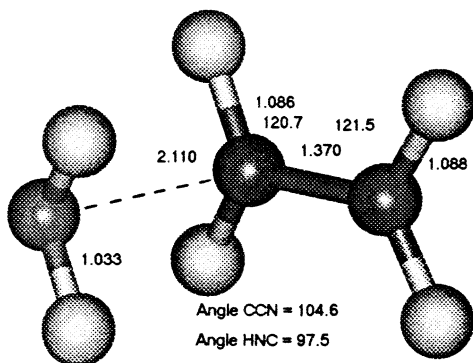


Fig. 11. Transition state for forming a $\text{CH}_2=\text{CH}_2 \cdots \text{NH}_2$ complex, or possibly for dissociation to $\text{CH}_2=\text{CH}_2 + \text{NH}_2$.

- (5) Symmetric ionized cyclopropanediol and cyclopropanone are low energy transition states rather than potential energy minima.

Acknowledgement

The authors thank Thomas Chen for invaluable assistance in setting up and operating the computer used in these studies.

References

- [1] J.J. Zwinselman, N.M.M. Nibbering, C.E. Hudson, D.J. McAdoo, *Int. J. Mass Spectrom. Ion Phys.* 46 (1983) 129.
- [2] D.J. McAdoo, C.E. Hudson, J.J. Zwinselman, N.M.M. Nibbering, *J. Chem. Soc. Perkin Trans. 2* (1985) 1703.
- [3] T. Weiske, H. Schwarz, *Chem. Ber.* 116 (1983) 323.
- [4] E. Göksu, T. Weiske, H. Halim, H. Schwarz, *J. Am. Chem. Soc.* 106 (1984) 1167.
- [5] T. Weiske, H. Halim, H. Schwarz, *Chem. Ber.* 118 (1985) 495.
- [6] T. Weiske, H. Schwarz, *Tetrahedron* 42 (1986) 6245.
- [7] L.B. Harding, *J. Am. Chem. Soc.* 103 (1981) 7469.
- [8] T. Caronna, A. Citterio, M. Ghirardini, F. Minisci, *Tetrahedron* 33 (1977) 793.
- [9] D.J. McAdoo, C.E. Hudson, T. Lin, L.L. Griffin, J.C. Traeger, *Int. J. Mass Spectrom. Ion Processes* 87 (1989) 61.
- [10] M.J. Frisch, G.W. Trucks, H.B. Schlegel, P.M.W. Gill, B.G. Johnson, M.A. Robb, J.R. Cheeseman, T. Keith, G.A. Petersson, J.A. Montgomery, K. Raghavachari, M.A. Al-Laham, V.G. Zakrzewski, J.V. Ortiz, J.B. Foresman, J. Cioslowski, B.B. Stefanov, A. Nanayakkara, M. Challacombe, C.Y. Peng, P.Y. Ayala, W. Chen, M.W. Wong, J.L. Andres, E.S. Replogle, R. Gomperts, R.L. Martin, D.J. Fox, J.S. Binkley, D.J. Defrees, J. Baker, J.P. Stewart, M. Head-Gordon, C. Gonzalez, J.A. Pople, GAUSSIAN 94, revision E.2, Gaussian, Inc., Pittsburgh, PA, 1995.
- [11] J. Frisch, G.W. Trucks, H.B. Schlegel, G.E. Scuseria, M.A. Robb, J.R. Cheeseman, V.G. Zakrzewski, J.S.A. Montgomery, Jr., R.E. Stratmann, J.C. Burant, S. Dapprich, J.M. Millam, A.D. Daniels, K.N. Kudin, M.C. Strain, O. Farkas, J. Tomasi, V. Barone, M. Cossi, R. Cammi, B. Mennucci, C. Pomelli, C. Adamo, S. Clifford, J. Ochterski, G.A. Petersson, P.Y. Ayala, Q. Cui, K. Morokuma, D.K. Mallick, A.D. Rabuck, K. Raghavachari, J.B. Foresman, J. Cioslowski, J.V. Ortiz, A.G. Baboul, B.B. Stefanov, G. Liu, A. Liashenko, P. Piskorz, I. Komaromi, R. Gomperts, R.L. Martin, D.J. Fox, T. Keith, M.A. Al-Laham, C.Y. Peng, A. Nanayakkara, M. Challacombe, P.M.W. Gill, B. Johnson, W. Chen, M.W. Wong, J.L. Andres, C. Gonzalez, M. Head-Gordon, E.S. Replogle, J.A. Pople, GAUSSIAN 98, revision A.9, Gaussian, Inc., Pittsburgh, PA, 1998.
- [12] A.P. Scott, L. Radom, *J. Phys. Chem.* 100 (1996) 16502.
- [13] D.J. McAdoo, D.N. Witiak, F.W. McLafferty, *J. Am. Chem. Soc.* 99 (1977) 7265.

- [14] D.J. McAdoo, D.N. Witiak, F.W. McLafferty, J.D. Dill, *J. Am. Chem. Soc.* 100 (1978) 6639.
- [15] D.J. McAdoo, D.N. Witiak, *Org. Mass Spectrom.* 13 (1978) 499.
- [16] C.E. Hudson, D.J. McAdoo, *Org. Mass Spectrom.* 17 (1982) 366.
- [17] M.J. Polce, C. Wesdemiotis, *J. Am. Soc. Mass Spectrom.* 7 (1996) 573.
- [18] G. Bouchoux, A. Luna, J. Tortajada, *Int. J. Mass Spectrom. Ion Processes* 167/168 (1997) 353.
- [19] F. Turecek, V. Hanus, T. Gaumann, *Int. J. Mass Spectrom. Ion Processes* 69 (1986) 217.
- [20] J.C. Traeger, C.E. Hudson, D.J. McAdoo, *Org. Mass Spectrom.* 24 (1989) 230.
- [21] R.L. Smith, K.K. Thoen, K.M. Stirk, J.I. Kenttämä, *Int. J. Mass Spectrom. Ion Processes* 165/166 (1997) 315.
- [22] C.E. Hudson, D.J. McAdoo, *Tetrahedron* 46 (1990) 331.
- [23] D.J. McAdoo, C.E. Hudson, F.W. McLafferty, T.E. Parks, *Org. Mass Spectrom.* 19 (1984) 353.
- [24] C. Walling, in *Molecular Rearrangements*, P. De Mayo (Ed.), Interscience, New York, 1963, p. 407.
- [25] S.G. Lias, J.E. Bartmess, J.F. Liebman, J.L. Holmes, R.D. Levin, W.G. Mallard, *J. Chem. Phys. Ref. Data* 17 (1988).